Inorganic Chemistry

Article

pubs.acs.org/IC

Synthesis and Characterization of Molecular Hexagons and Rhomboids and Subsequent Encapsulation of Keggin-Type Polyoxometalates by Molecular Hexagons

Kazuhiro Uehara, Takamichi Oishi, Takayuki Hirose, and Noritaka Mizuno*

Department of Applied Chemistry, School of Engineering, The University of Tokyo, 7-3-1 Hongo, Bunkyo-ku, Tokyo 113-8656, Japan

Supporting Information

ABSTRACT: Structural control among hexagonal (trimer), rhomboidal (dimer), and infinite-chain supramolecular complexes with three different supporting ligands of ethylenediamine (en), *N*,*N*,*N*′,*N*′-tetramethylethylenediamine (en*), and 1,2-bis(diphenyl)-phosphinoethane (dppe) $[(en)Pd(L)]_3(OTf)_6$ **1t·OTf**, $[(en^*)Pd(L)]_2(PF_6)_4$ **2d·PF$_6$**, and $[(dppe)Pd(L)(OTf)_2]_\infty$ **3·OTf** (OTf = trifluoromethane sulfonate; L = 1,3-bis(4-pyridylethynyl)benzene) in the solid and solution states was investigated. The encapsulation of a large Keggin-type polyoxometalate $[\alpha\text{-}PW_{12}O_{40}]^{3-}$ by these complexes was also examined. As the steric bulkiness of the supporting ligands increased in the order of en < en* < dppe, the hexagonal, rhomboidal, and infinite-chain structures were obtained, as confirmed by X-ray crystallography. In solution, equilibrium between the molecular hexagon (**1t·OTf/2t·PF$_6$**) and the molecular rhomboid (**1d·OTf/2d·PF$_6$**) was observed in the en/en* ligand systems, whereas **3·OTf** with the dppe ligand did not exhibit equilibrium and instead existed as a single species. These phenomena were established by cold-spray ionization mass spectroscopy (CSI-MS) and ^{1}H diffusion ordered NMR spectroscopy (DOSY). The addition of the highly negatively charged Keggin-type phosphododecatungstate $[\alpha\text{-}PW_{12}O_{40}]^{3-}$ to a solution of **2t/2d·PF$_6$** resulted in the encapsulation of the tungstate species in the cavity of the molecular hexagon to form $\{[(en^*)Pd(L)]_3[\supset\alpha\text{-}PW_{12}O_{40}]\}(PF_6)_3$ **2t·**$[\alpha\text{-}PW_{12}O_{40}]^{3-}$, as confirmed by a combination of ^{1}H and ^{31}P DOSY and CSI-MS spectral data.

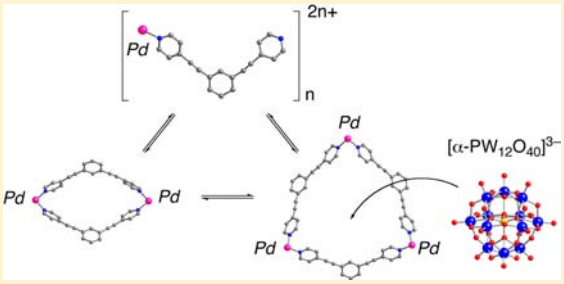

INTRODUCTION

The molecular recognition of specific chemical species using nanosized porous materials has attracted significant attention[1−3] because these materials may have applications in gas storage,[4] drug delivery,[5] catalysis,[6] molecular magnets,[7] molecular modification,[8] and anion transport.[9] To exploit molecular recognition in artificial systems, the use of supramolecules such as molecular polygons and polyhedra is preferable because such supramolecules typically possess large cavities with sizes and shapes that can be tuned by applying various bridging ligands.[10] Although hexagonal structures often occur in nature and can be observed in structures such as beehives, ice crystals, and chemical compounds including benzene and graphite,[11] hexagonal supramolecules are rare.[12] In 2003, Stang et al. reported the discovery of molecular hexagons and rhomboids consisting of M_nL_n units (M, metal complex fragment; L, bridging ligand; n = 2, 3) equilibrated in solution. Only the rhomboidal crystal structure of $[(Et_3P)_2Pt(L')]_2(PF_6)_4$ (L′ = 3,5-di(pyridylethynyl)pyridine) was observed during X-ray crystallography,[12a] although the existence of the molecular hexagon $[(Et_3P)_2Pt(L')]_3(PF_6)_6$ was confirmed by electron spray ionization mass spectrometry (ESI-MS) and nuclear magnetic resonance (NMR) spectroscopy. As a result of the limited data concerning molecular hexagons, significant effort has been applied to determining the structures of these compounds and to the detailed elucidation of their equilibrium properties.[13−23]

Polyoxometalates (POMs) are nanosized anionic metal-oxide clusters that exhibit thermal stability and are well suited for use as inorganic building blocks.[24] Many examples of inorganic−organic hybrid compounds based on transition-metal complexes and POMs have been reported to date, whereas combinations of discrete supramolecules and POMs are still rare.[24g,25] Previously, we have reported the encapsulations of a hexatungstate $[W_6O_{19}]^{2-}$ and a decatungstate $[W_{10}O_{32}]^{4-}$ into the molecular square $[(en^*)Pd(4,4'\text{-bpy})]_4(NO_3)_8$ (en* = *N*,*N*,*N*′,*N*′-tetramethylethylenediamine and 4,4′-bpy = 4,4′-bipyridine) to form $\{[(en^*)Pd(4,4'\text{-bpy})]_4[\supset W_6O_{19}]\}(NO_3)_4$ and $\{[(en^*)Pd(4,4'\text{-bpy})]_4[\supset W_{10}O_{32}]\}[W_{10}O_{32}]$, respectively.[23a] The encapsulation of POMs takes place only in cases where the size and symmetry of the POM corresponds to those of the cavity of the molecular square. Therefore, a larger sized supramolecule with a cavity possessing C_3 or C_6 symmetry would be required to encapsulate nanosized Keggin-type POMs.

In this Article, structural control in the solid state between hexagonal, rhomboidal, and infinite-chain supramolecules

Received: June 8, 2013
Published: September 19, 2013

dx.doi.org/10.1021/ic401428v | *Inorg. Chem.* 2013, 52, 11200−11209

through tuning the steric hindrance of the three different supporting ligands ethylenediamine (en), *N,N,N′,N′*-tetramethylethylenediamine (en*), and 1,2-bis(diphenylphosphino)-ethane (dppe) was studied. The encapsulation of the negatively charged Keggin-type phosphododecatungstate $[\alpha\text{-}PW_{12}O_{40}]^{3-}$ in the cavity of the molecular hexagon in solution was also investigated using the pulse-field gradient echo (PFGE) NMR technique.[26−28]

RESULTS AND DISCUSSION

Synthesis and Characterization of Molecular Hexagon (Trimer), Rhomboid (Dimer), and Infinite-Chain Supramolecules, $[(L_m)Pd(L)]_n(X)_{2n}$ (n = 2, 3, and ∞). A series of supramolecular compounds was synthesized via the dechlorination of $(L_m)PdCl_2$ (L_1 = ethylenediamine (en) and L_2 = *N,N,N′,N′*-tetramethylethylenediamine (en*)) with AgX (X = OTf^- or PF_6^-) followed by the reaction of the resulting $[(L_m)Pd(solv.)_2]_n(X)_{2n}$ with 1,3-bis(4-pyridylethynyl)benzene (L) in CH_3CN (Scheme 1). Pale-yellow products consisting of

Scheme 1

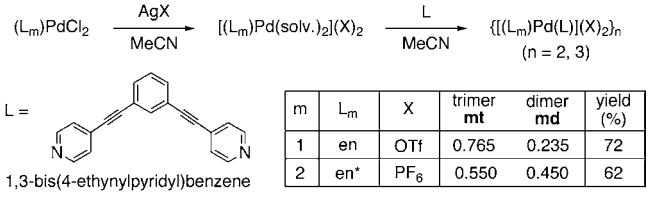

m	L_m	X	trimer **mt**	dimer **md**	yield (%)
1	en	OTf	0.765	0.235	72
2	en*	PF_6	0.550	0.450	62

1t·OTf (72% yield) or **2d·PF_6** (62% yield) were obtained by recrystallization from a solvent mixture of $MeNO_2$ and Et_2O. The successful complexations of $[(L_m)Pd(L)(X)_2]_n$ (**1t·OTf**: L_m = en and X = OTf^-; **2d·PF_6**: L_m = en* and X = PF_6^-) were confirmed by infrared spectroscopy (IR), NMR (^1H, ^{13}C, ^{19}F, ^{31}P, and HMQC), cold-spray ionization mass spectroscopy (CSI-MS), and elemental analyses, whereas molecular structures were determined by X-ray crystallography (Figure 1). The crystallographic data and selected bond distances and angles are summarized in Tables 1 and 2.

Compound **1t·OTf** was isolated as a molecular hexagon, $[(en)Pd(L)(OTf)_2]_3$, which crystallized in the $P\bar{3}$ space group with a C_3 axis along the principle c axis (Figure 1a). All of the anions were located near the palladium center and were outside the cavity of the molecular hexagon. Each intramolecular Pd···Pd distance was 17.963 Å. In the crystal lattice of **1t·OTf**, three neighboring molecular hexagons interact with each other at the phenyl rings via $\pi-\pi$ stacking interactions (3.645 Å, Figure 2), and hexagonal columns with layer distances of 8.587 Å are built up along the c-axis.

In contrast, compound **2d·PF_6** was isolated as a molecular rhomboid, $[(en^*)Pd(L)]_2(PF_6)_2$, which crystallized in the $P\bar{1}$ space group and consisted of two crystallographically independent rhomboidal molecules (Figure 1b). The structure of the cationic moiety is analogous to that of $[(Et_3P)_2Pt(L')]_2(PF_6)_4$, as reported by Stang et al.[12a] The hexafluorophosphate anions were located near the palladium center and outside the cavity. Their diagonal Pd···Pd distances were 16.265 and 16.185 Å, respectively. Two crystallographically independent molecules were stacked at the phenyl and pyridyl rings through $\pi-\pi$ stacking interactions whose closest distance (C(Ph)···C(Py)) was calculated to be 3.751 Å. Rhomboidal columnar channels along the a axis with layer distances of 9.994 Å are formed in the crystal lattice (Figure 3).

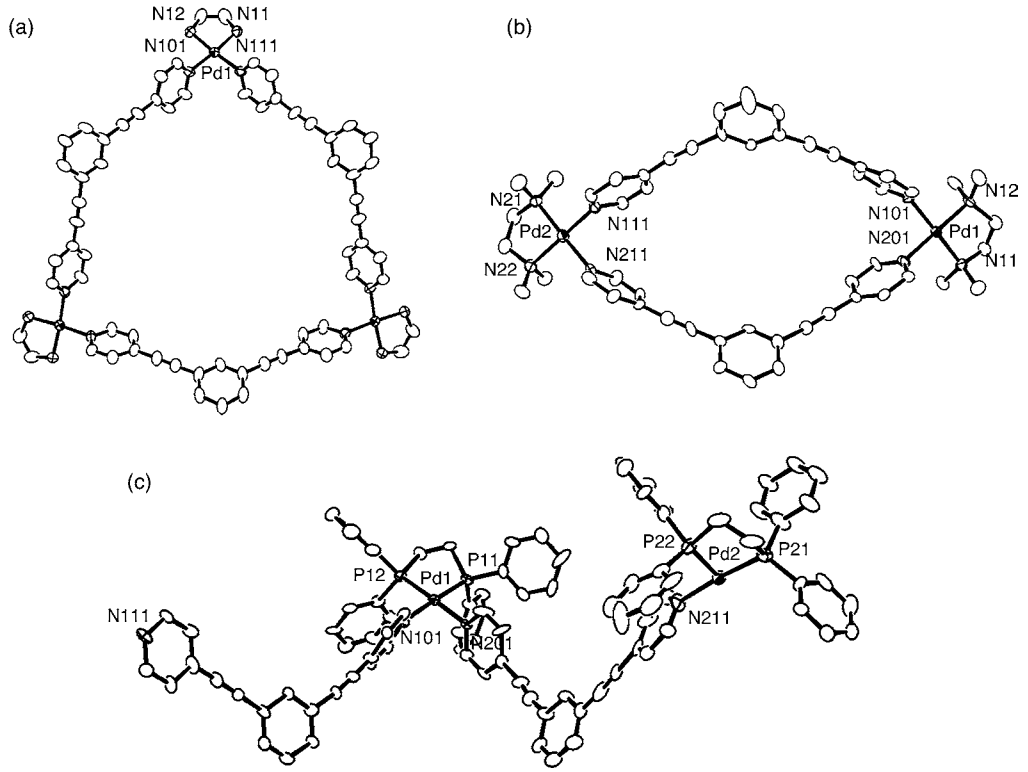

Figure 1. ORTEP views of (a) $[(en)Pd(L)]_3(OTf)_6$ **1t·OTf**, (b) $[(en^*)Pd(L)]_2(PF_6)_4$ **2d·PF_6** and (c) $\{(dppe)Pd(L)[W_6O_{19}]\}_\infty$ **3·W_6O_{19}** at the 30% probability level. Anionic moieties are omitted for clarity.

dx.doi.org/10.1021/ic401428v | *Inorg. Chem.* 2013, 52, 11200−11209

Table 1. Crystallographic Data for 1t·OTf, 2d·PF_6, and 3·W_6O_{19}

	1t·OTf	2d·PF_6	3·W_6O_{19}
empirical formula	$C_{66}H_{60}N_{12}Pd_3$	$C_{104}H_{104}N_{16}Pd_4$	$C_{92}H_{62}N_4O_{38}P_4Pd_2W_{12}$
formula weight	1340.5433	1001.82	4384.42
crystal system	trigonal	triclinic	monoclinic
lattice type	primitive	primitive	C-centered
space group	$P\bar{3}$ (No. 147)	$P\bar{1}$ (No. 2)	$C2/c$ (No. 15)
lattice parameter	a = 30.4650(10) Å	a = 19.7695(9) Å	a = 57.0002(8) Å
		b = 21.0669(9) Å	b = 17.0179(3) Å
	c = 8.7859(4) Å	c = 24.6332(15) Å	c = 34.8057(7) Å
		α = 99.229(2)°	
		β = 92.209(3)°	β = 122.5000(10)°
	γ = 120°	γ = 117.576(4)°	
	V = 7061.9(5) Å^3	V = 8901.2(8) Å^3	V = 28474.9(9) Å^3
Z	2	2	8
d_{calcd}	0.63 g cm^{-3}	0.751 g cm^{-3}	2.045 g cm^{-3}
F_{000}	1356	2064	15 968
μ(Mo Kα)	0.40 mm^{-1}	0.427 mm^{-1}	10.001 mm^{-1}
no. of reflections measured	13 068	43 946	39 328
no. of observations	5695	12 442	20 784
no. of variables	244	973	745
R_1[a]	0.0678	0.1077	0.0931
wR_2[a]	0.221	0.2892	0.2955

[a] $I > 2.00\sigma(I)$.

Table 2. Selected Bond Distances (Angstroms) and Angles (Degrees) of 1t·OTf, 2d·PF_6, and 3·W_6O_{19}

		2d·PF_6		
	1t·OTf	compound A	compound B	3·W_6O_{19}
Pd–X(L_m)	2.017(3), 2.012(3)	2.064(8), 2.083(7)	2.114(8), 2.054(8)	2.257(4), 2.263(4)
		2.097(7), 2.112(8)	2.109(8), 2.112(8)	2.249(4), 2.251(5)
Pd–L(Py)	2.031(3), 2.040(3)	2.043(4), 2.036(5)	2.042(5), 2.050(5)	2.122(5), 2.063(6)
		2.026(4), 2.033(4)	2.035(4), 2.043(5)	2.075(7), 2.079(7)
X(L_m)–Pd–X(L_m)	84.50(14)	85.9(3), 85.8(3)	84.2(4), 86.7(3)	84.3(5), 85.1(2)
X(L_m)–Pd–L(Py)	91.92(13), 91.16(14)	95.1(3), 95.2(3)	94.6(3), 95.5(3)	94.0(3), 96.4(2)
		95.2(3), 95.5(3)	93.8(3), 95.1(3)	92.0(3), 94.7(3)
L(Py)–Pd–L(Py)	92.40(13)	85.0(2), 83.5(2)	85.7(2), 84.5(2)	85.1(3), 88.1(4)
Pd···Pd	17.969	16.265	16.185	16.628

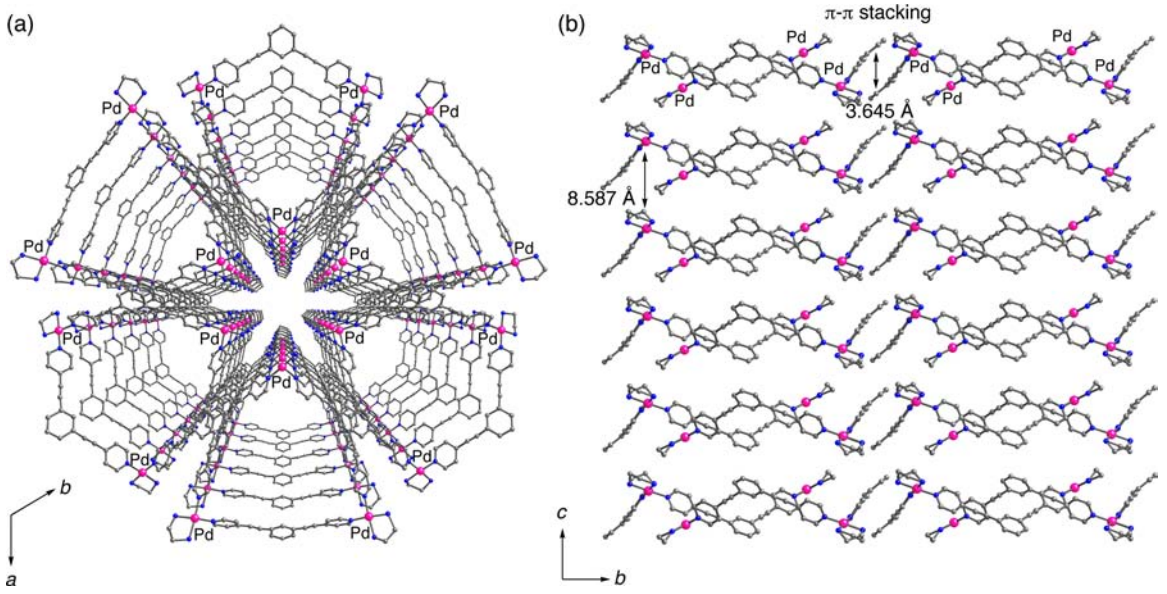

Figure 2. Crystal packing of **1t·OTf** viewed along the (a) c axis and (b) a axis.

dx.doi.org/10.1021/ic401428v | Inorg. Chem. 2013, 52, 11200−11209

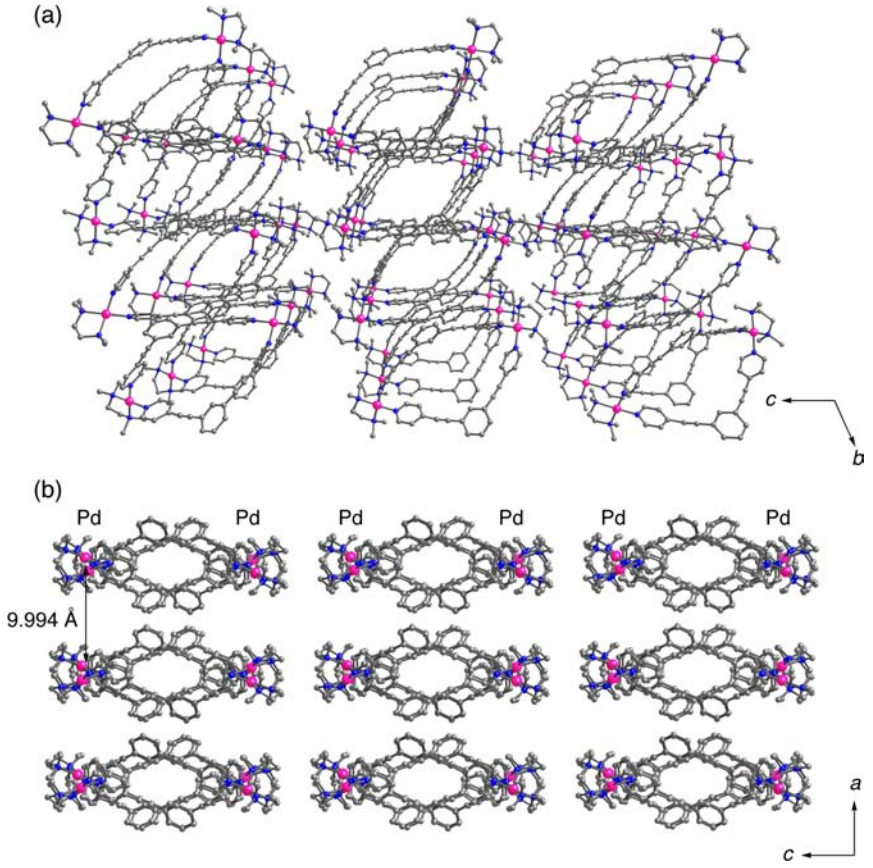

Figure 3. Crystal packing of **2d·PF$_6$** viewed along the (a) *a* axis and (b) *b* axis.

Employing the more highly sterically hindered 1,2-bis(diphenylphosphino)ethane (dppe) supporting ligand disallowed the formations of the molecular hexagon or rhomboid and instead resulted in the formation of $[(dppe)Pd(L)(OTf)_2]_\infty$ (**3·OTf**, 95% yield). A single crystal suitable for X-ray crystallography was successfully obtained as a hexatungstate derivative by anion exchange with $(TBA)_2[W_6O_{19}]$ (TBA = tetra(*n*-butyl)ammonium).[29] X-ray crystallography demonstrated the formation of an infinite-chain complex $\{(dppe)Pd(L)[W_6O_{19}]\}_\infty$ **3·W$_6$O$_{19}$** (Figure 1c). The X(L_m)−Pd−L(Py) angles (92.0(3)−96.4(2)°) were relatively wide compared to those of **1t·OTf** and were comparable to those of **2d·PF$_6$** (Table 2). The steric repulsion between the supporting ligand (dppe) and the bridging ligand (L) in **3·W$_6$O$_{19}$** generates these wider angles. Because the L(Py)−Pd−L(Py) angles (85.1(3) and 88.1(4)°) were also wider than or comparable to those of **2d·PF$_6$** (83.5(2)−85.7(2)°), **3·W$_6$O$_{19}$** (having the bulkier dppe supporting ligand) does not adopt the rhomboidal structure but instead forms the infinite-chain structure to decrease the steric repulsion between neighboring bridging ligands. These results show that steric hindrance between the supporting and bridging ligands is one of the most important factors controlling the resultant solid-state structures.

Steric Effects on the Supramolecular Structures. The steric effects between supporting and bridging ligands on the supramolecular structure have been discussed in our previous report on the equilibrium between molecular square and triangle structures.[23b] The Pd−X(L_m) (2.017(3) and 2.012(3) Å) and Pd−L(Py) distances (2.031(3) and 2.040(3) Å) in **1t·OTf** were shorter than or comparable to those in **2d·PF$_6$** (Pd−X(L_m), 2.054(8)−2.114(8) Å and Pd−L(Py), 2.026(4)−2.050(5) Å), suggesting the weak coordination of ligands in **2d·PF$_6$**. Similarly, the L(Py)−Pd−L(Py) angles in **1h·OTf** (92.40(13)°) were wider than those in **2d·PF$_6$** (83.5(2)−85.7(2)°), whereas the X(L_m)−Pd−L(Py) angles in **1h·OTf** (91.92(13) and 91.16(14) Å) were narrower than those of **2d·PF$_6$** (93.8(3)−95.5(3)°). These results indicate that close contact between the methyl substituents of the en* supporting ligand and the bridging ligand (L) are avoided. The effects of steric interactions were also observed in the ^{1}H NMR spectra of these structures. The Py(α) and Py(β) signals of **1t·OTf** (8.81 and 7.81 ppm) and **2t·PF$_6$** (9.19 and 7.84 ppm) were observed at lower magnetic-field positions than those of **1d·OTf** (8.70 and 7.78 ppm) and **2d·PF$_6$** (9.13 and 7.78 ppm), respectively. Because the cavity of the molecular rhomboid is narrower than that of the hexagon, it follows that the magnetic shielding of the molecular rhomboid will be greater than that of the hexagon. The most prominent difference was that the signal at the 2 position of the phenyl ring in **1t·OTf** was observed at 7.88 ppm, whereas that of **1d·OTf** was shifted upfield (7.54 ppm). In the case of the supporting ligand, however, the shift tendency was different from that of the bridging ligand. Because the X(L_m)−Pd−L(Py) angles in **2t·PF$_6$** were wider than those in **2d·PF$_6$**, as might be predicted from the **1t·OTf** spectra, the signal corresponding to the methyl substituents in **2t·PF$_6$** (2.63 ppm) was shifted downfield compared to that of **2d·PF$_6$** (2.55 ppm).

Behaviors of Molecular Hexagons and Rhomboids in Solution. The CSI-MS spectra of **1t·OTf** and **2d·PF$_6$** exhibited peaks at m/z = 1340.88 and 2085.78, assignable to $\{[(en)Pd(L)]_n(OTf)_{2n-1}\}^+$, and at m/z = 1441.04 and 2233.01, assignable to $\{[(en^*)Pd(L)]_n(PF_6)_{2n-1}\}^+$ (n = 2, 3) (Figures

dx.doi.org/10.1021/ic401428v | *Inorg. Chem.* 2013, 52, 11200−11209

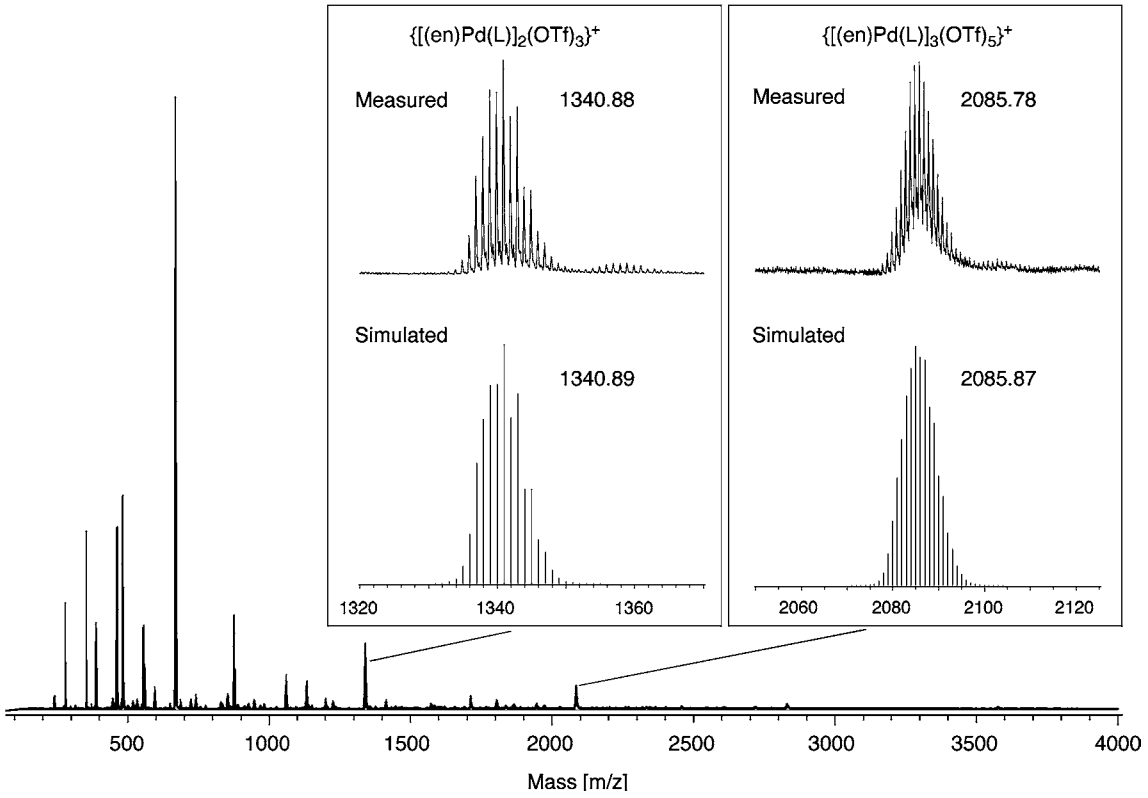

Figure 4. CSI-MS spectrum of $[(en)Pd(L)]_n(OTf)_{2n}$ **1t/1d·OTf** (n = 2, 3).

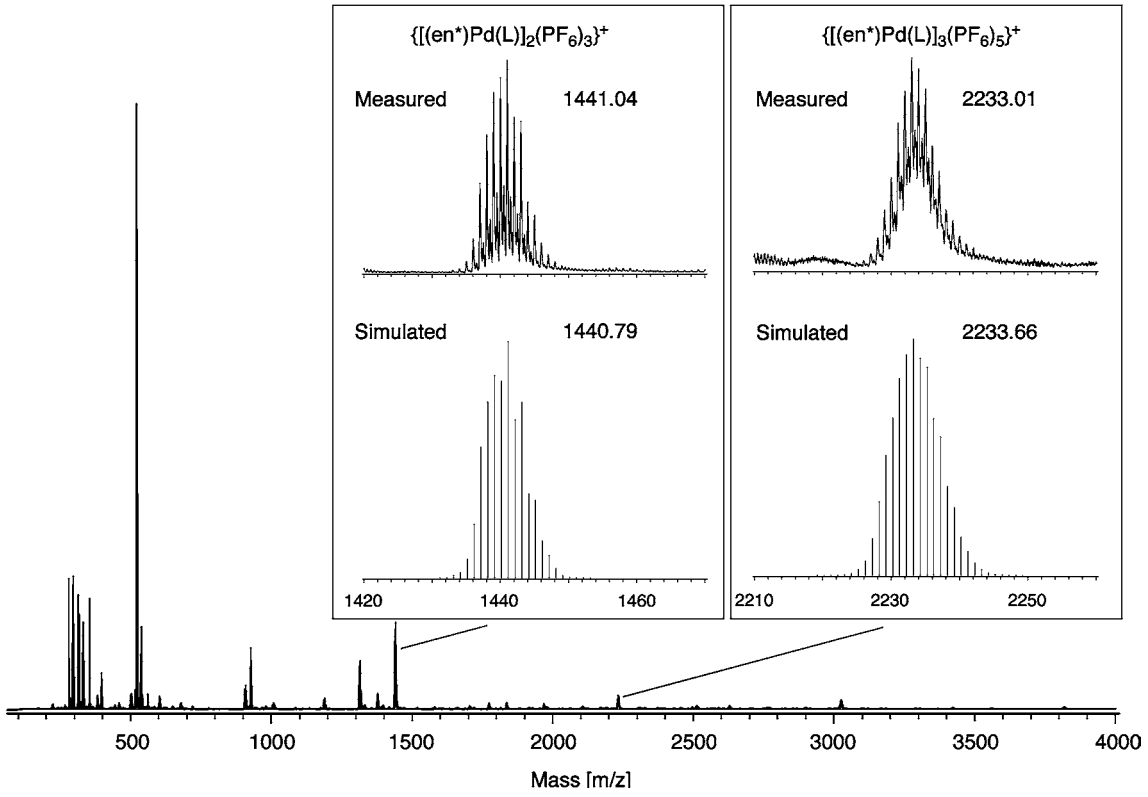

Figure 5. CSI-MS spectrum of $[(en^*)Pd(L)]_n(PF_6)_{2n}$ **2t/2d·PF$_6$** (n = 2, 3).

4 and 5). The ^{1}H NMR spectra of **1t/1d·OTf** and **2t/2d·PF$_6$** (5 mM) exhibited two sets of signals (**1t·OTf/1d·OTf** = 0.765:0.235 in DMSO-d_6 at 298 K) and **2t/2d·PF$_6$** (**2t·OTf/2d·OTf** = 0.550:0.450 in DMSO-d_6 at 298 K). The behaviors of **1t/1d·OTf** and **2t/2d·PF$_6$** in solution were confirmed using the pulse-field gradient echo (PFGE) NMR technique. ^{1}H diffusion ordered NMR spectroscopy (DOSY) of **1t/1d·OTf** revealed that the diffusion coefficients of **1t·OTf** and **1d·OTf** in **1t/1d·**

dx.doi.org/10.1021/ic401428v | *Inorg. Chem.* 2013, 52, 11200−11209

OTf at 303 K were 6.23(1) × 10^{-11} and 8.95(1) × 10^{-11} m^2 s^{-1}, respectively, and the corresponding effective molecular radii (R_{eff}) were 1.83 and 1.25 nm, respectively, on the basis of the Stokes–Einstein equation (Table 3 and Figures S9–S11 in the Supporting Information). The R_{eff} of **1t/1d·OTf** was slightly larger than those of the molecular hexagon (1.46 nm) and rhomboid (1.31 nm), as determined by DFT calculations (Figure 6).[25] On the contrary, the diffusion coefficients of **2t·PF_6** and **2d·PF_6** in **2t/2d·PF_6** at 303 K were 7.58(5) × 10^{-11} and 1.06(7) × 10^{-10} m^2 s^{-1}, respectively, and the corresponding R_{eff} were 1.48 and 1.06 nm (Figures S13–S15 in the Supporting Information) and thus were slightly smaller than those of **1t/1d·OTf**. These results indicate that **2t/2d·PF_6** in solution also exists as the molecular hexagon (1.46 nm) and rhomboid (1.29 nm). As the solution temperature is increased, the **1d·OTf** and **2d·PF_6** signals increase in intensity because of entropic effects on the systems. Similarly, as the concentration of the molecular rhomboid increases, the molecular hexagon signals increase in accordance with Le Châtelier's principle. The behaviors of these substances are consistent with those observed in previous work with regard to the equilibrium between the molecular square and triangle.

Table 3. Diffusion Coefficients Obtained from Diffusion Ordered NMR Spectroscopy (DOSY) in DMSO-d_6 at 303 K

	diffusion coefficient, D (10^{-10} m^2 s^{-1})		stokes radius (r nm^{-1})[a]	
compound	^{1}H	^{31}P/^{19}F	cation	anion
1t·OTf	0.623(1)	1.5(1)[b]	1.83	0.747
1d·OTf	0.895(1)		1.25	
2t·PF_6	0.758(5)	6.99(3)[c]	1.48	0.160[b]
2d·PF_6	1.06(7)		1.06	
3·OTf	1.76(2)	2.73(4)[b]	0.637	0.411
2t·[α-$PW_{12}O_{40}$]$^{3-}$	0.724(3)	0.736(3)[d]	1.55	1.52[d]
2d·[α-$PW_{12}O_{40}$]$^{3-}$	1.05(3)		1.06	
H_3[α-$PW_{12}O_{40}$]		1.90 (3)		0.590

[a]Obtained from the Stokes–Einstein equation $r = kT/(6\pi\eta D)$ (k = Boltzmann constant and η = viscosity (0.00198 for DMSO) (g m^{-1} s^{-2})). [b]The value derived from OTf^-. [c]The value derived from PF_6^-. [d]The value derived from [α-$PW_{12}O_{40}$]$^{3-}$.

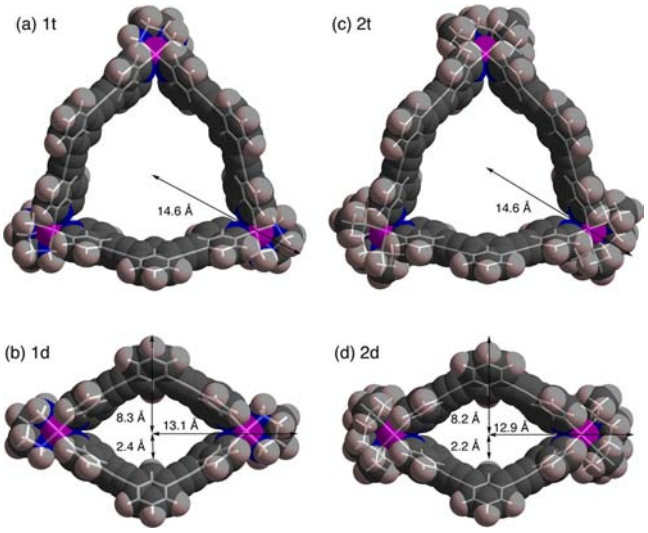

Figure 6. Space-filling models of the cationic moieties of the molecular hexagon and rhomboid as optimized by DFT calculations: (a) **1t**, (b) **1d**, (c) **2t**, and (d) **2d**.

In the ^{1}H NMR spectra of **3·OTf**, only a single set of signals was observed, suggesting no equilibrium in solution. The diffusion coefficient of **3·OTf** was calculated to be 1.76(2) × 10^{-10} m^2 s^{-1}, and the corresponding R_{eff} is 0.637 nm (Figures S17 in the Supporting Information). On the basis of these results, infinite-chain compound **3·OTf** likely exists in solution as a mononuclear species such as [(dppe)Pd(L)(solvent)]-$(OTf)_2$. The CSI-MS spectrum of **3·OTf** exhibited peaks at m/z = 934.09 that are attributed to {[(dppe)Pd(L)](OTf)}$^+$, providing support for this theory (Figure S5 in the Supporting Information). In addition, the diffusion coefficients for trifluoromethane sulfonate (OTf^-) and hexafluorophosphate (PF_6^-) were calculated to be 1.5(1) × 10^{-10} for **1t/1d·OTf**, 2.73(4) × 10^{-10} for **3·OTf**, and 6.99(3) × 10^{-10} m^2 s^{-1} for **2t/2d·PF_6**, and the corresponding R_{eff} were 0.747, 0.411, and 0.160 nm, respectively (Figures S12, S16, and S18 in the Supporting Information). These radii are almost in agreement with those (ca. 0.275 and 0.174 nm) obtained from DFT calculations.[30,31] Because the diffusion coefficients of cationic and anionic moieties are quite different, the electrostatic interactions between the cationic ring and the counteranions are considered to be very weak.

Encapsulation of a Keggin-Type Polyoxometalate in the Molecular Hexagon Cavity. To confirm the ability of the molecular hexagon to encapsulate POMs, reactions of **1t·OTf** and **2d·PF_6** with H_3[α-$PW_{12}O_{40}$] were carried out. Unfortunately, because this reaction generated a product that was only sparingly soluble in the case of **1t·OTf**, no information concerning the encapsulation of [α-$PW_{12}O_{40}$]$^{3-}$ in the **1t·OTf** cavity was obtained. However, the reaction of **2d·PF_6** with H_3[α-$PW_{12}O_{40}$] at a 1:1 molar ratio in DMSO-d_6 resulted in the successful encapsulation of [α-$PW_{12}O_{40}$]$^{3-}$ in the cavity of **2t** to form {[(en*)Pd(L)]$_3$⊃[α-$PW_{12}O_{40}$]}$(PF_6)_3$ **2t·**[α-$PW_{12}O_{40}$]$^{3-}$. ^{1}H DOSY NMR spectra demonstrated that the diffusion coefficients of **2t/2d·**[α-$PW_{12}O_{40}$]$^{3-}$ were 0.724(3) × 10^{-10} (R_{eff}, 1.55 nm) and 1.05(3) × 10^{-10} (R_{eff}, 1.06 nm) m^2 s^{-1} (Figures S19–S21 in the Supporting Information). The diffusion coefficients of **2t/2d·**[α-$PW_{12}O_{40}$]$^{3-}$ were almost identical to those of **2t/2d·PF_6** after the complexation between **2t/2d·PF_6** and H_3[α-$PW_{12}O_{40}$].

Subsequent to encapsulation, the signals of the molecular rhomboid decreased, whereas those of the corresponding molecular hexagon appeared, as shown in Figure 7. The protons at the 2 position of the phenyl moiety on the bridging ligand (at 7.78 ppm) are evidently shifted to a lower magnetic field region (7.89 ppm), likely because these protons are in close proximity to the [α-$PW_{12}O_{40}$]$^{3-}$ ion and thus interact with the ion via hydrogen bonding. The ^{31}P{H}NMR spectra shows a peak at −14.34 ppm, which is lower than that of pure H_3[α-$PW_{12}O_{40}$] (−14.36 ppm), also suggesting slight deshielding resulting from complexation with highly charged molecular hexagon **2t**. The in situ CSI-MS spectra showed a primary peak at m/z = 4675.98, assignable to the molecular hexagon complex {[(en*)Pd(L)]$_3$[α-$PW_{12}O_{40}$]$(PF_6)_2$}$^+$ (m/z = 4675.52), whereas a peak originating from the molecular rhomboid complex {[(en*)Pd(L)]$_2$[α-$PW_{12}O_{40}$]}$^+$ (m/z = 3365.98) was not observed (Figure 8). Although a single crystal of the product could not be obtained, the product composition was deduced as [(en*)Pd(L)]$_3$[α-$PW_{12}O_{40}$]$(PF_6)_3$ on the basis of MS data together with the results of elemental analysis. In addition, we determined from ^{31}P DOSY NMR spectra that the diffusion

dx.doi.org/10.1021/ic401428v | Inorg. Chem. 2013, 52, 11200–11209

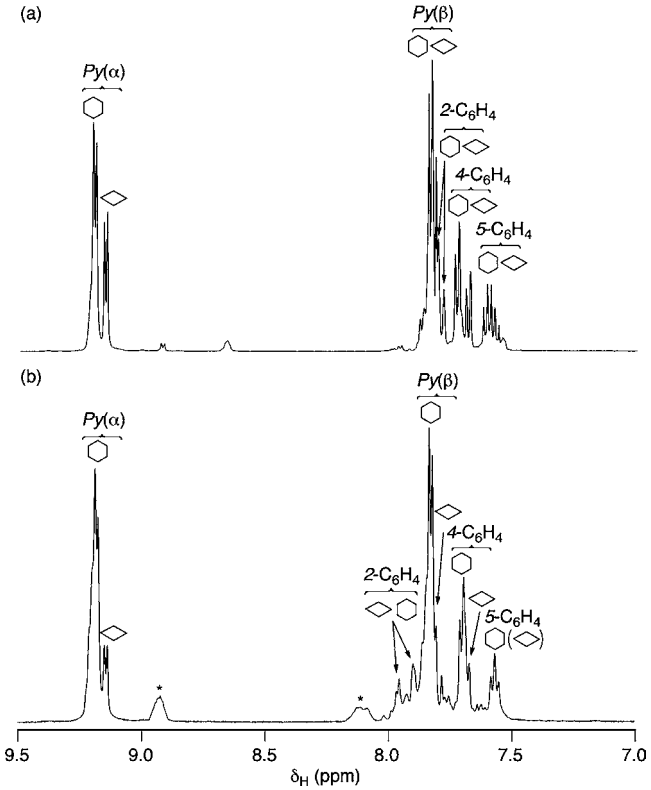

Figure 7. ^{1}H NMR spectra of (a) $[(en^*)Pd(L)]_2(PF_6)_4$ **2t/2d·PF$_6$** and (b) **2t/2d·PF$_6$** in the presence of $H_3[\alpha\text{-}PW_{12}O_{40}]$ (asterisks represent peaks derived from unknown species or solvent).

coefficient of the $[\alpha\text{-}PW_{12}O_{40}]^{3-}$ moiety was $7.36(3) \times 10^{-11}$ $m^2\ s^{-1}$, whereas the corresponding molecular radius was calculated to be 1.52 nm (Figure S22 in the Supporting Information). The diffusion coefficients of **2t** and $[\alpha\text{-}PW_{12}O_{40}]^{3-}$ were practically identical, which suggests that **2t** and $[\alpha\text{-}PW_{12}O_{40}]^{3-}$ interact with each other and that $[\alpha\text{-}PW_{12}O_{40}]^{3-}$ is encapsulated in the cavity of **2t** to form $\{[(en^*)Pd(L)]_3[\supset\alpha\text{-}PW_{12}O_{40}]\}(PF_6)_3$. Molecular dynamics calculations concerning the $\{[(en^*)Pd(L)]_3[\supset\alpha\text{-}PW_{12}O_{40}]\}^{3+}$ **2t**·$[\alpha\text{-}PW_{12}O_{40}]^{3-}$ complex using universal force field (UFF) parameters also indicated that the molecular hexagon encapsulates the Keggin-type POM while maintaining the framework of **2t** intact (Figure 9).

CONCLUSIONS

We have demonstrated that the structural control of hexagonal, rhomboidal, and infinite-chain complexes through the application of three different supporting ligands is attainable and that steric hindrance between the supporting and bridging ligands is the most important factor in determining the resulting solid-state structure. On the basis of data obtained from ^{1}H and ^{31}P DOSY NMR spectra, we also conclude that the internal cavity of the hexagonal structure possesses an adequate size and the appropriate symmetry to allow the successful encapsulation of $[\alpha\text{-}PW_{12}O_{40}]^{3-}$ in solution.

EXPERIMENTAL SECTION

Compound manipulations were carried out using standard Schlenk techniques under argon. The ligands 1,3-bis(4-pyridylethynyl)benzene (L), $(L_n)PdCl_2$ (L_n = ethylenediamine, *N*,*N*,*N*′,*N*′-tetramethylethylenediamine (en*), and 1,2-bis(diphenylphosphino)ethane) were synthesized according to procedures in the literature.[32,33] Tetrahydrofuran (THF) was distilled with $NaK_{2.8}$ under argon, and acetonitrile was distilled with P_2O_5 under argon. Dodecaphosphotungstic acid ($H_3[\alpha\text{-}PW_{12}O_{40}]$), diethylamine, nitromethane, diethylether, *n*-hexane, and DMSO-d_6 were used as-received. ^{1}H (270 MHz), ^{13}C{H} (67.8 MHz), ^{31}P{H} (109.25 MHz), and ^{19}F (465.89 MHz) NMR spectra were recorded on a JEOL ECA-500. Infrared spectra were acquired on a JASCO FT-IR 580, and CSI-MS spectra were obtained with a JEOL T100-CS. Elemental analysis was performed with a LECO CHNS-932 VTF-900.

Synthesis of $[(en)Pd(L)]_n(OTf)_{2n}$ 1t/1d·OTf (1t, *n* = 3; 1d, *n* = 2). The starting material $(en)PdCl_2$ (0.169 g, 0.712 mmol) was dissolved in MeCN (10 mL) followed by the addition of 2 equiv of AgOTf (0.367 g, 1.43 mmol). After the solution was stirred for 2 h, the

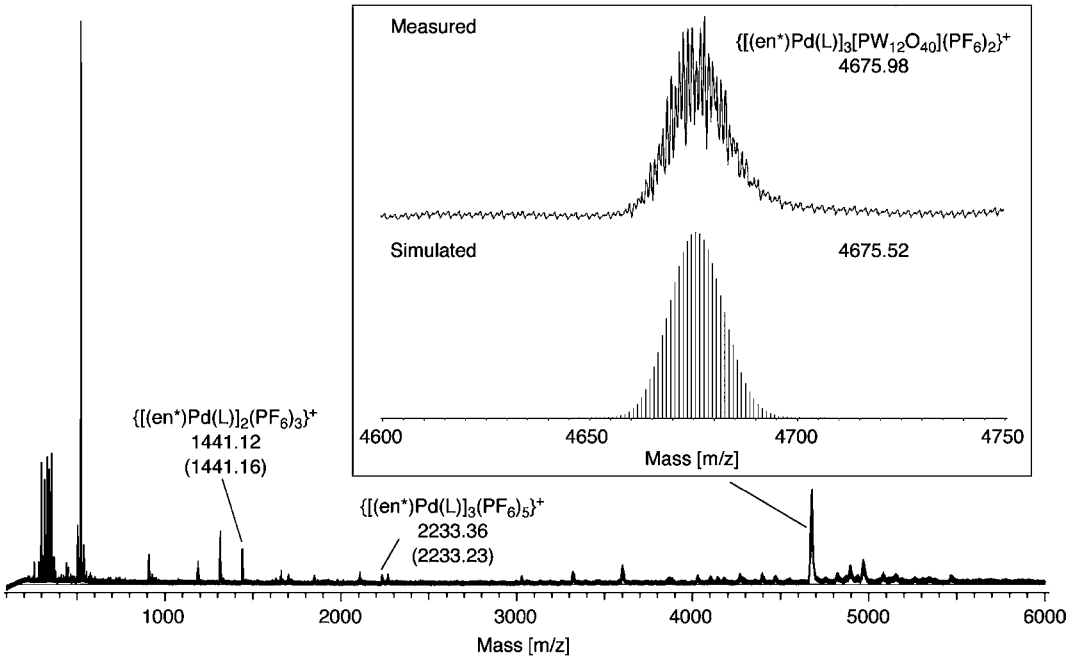

Figure 8. In situ CSI-MS spectrum of **2t/2d·PF$_6$** in the presence of $H_3[\alpha\text{-}PW_{12}O_{40}]$ in DMF (263 K).

dx.doi.org/10.1021/ic401428v | Inorg. Chem. 2013, 52, 11200−11209

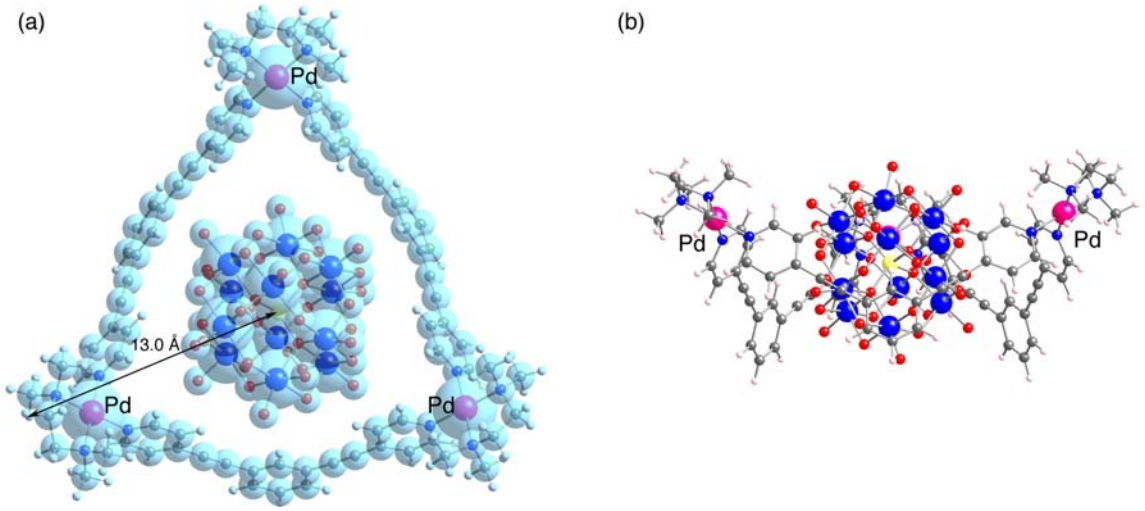

Figure 9. Molecular structure of $\{[(en^*)Pd(L)]_3[\supset\alpha\text{-}PW_{12}O_{40}]\}^{3+}$ **2t**·$[\alpha\text{-}PW_{12}O_{40}]^{3-}$ optimized by molecular dynamics with UFF: (a) top and (b) side views.

resulting AgCl was removed by filtration. The bridging ligand 1,3-bis(4-pyridylethynyl)benzene (L; 0.200 g, 0.713 mmol) was added to the filtrate, and the mixture was stirred overnight. The solvent was removed by evaporation. The crude product was dissolved in nitromethane, and the residual solid was centrifuged and recrystallized from nitromethane/Et_2O to give pale-green crystals of **1t·OTf** (0.382 g, 0.171 mmol, 72% yield). IR (KBr, cm^{-1}): 3234 m (ν(N−H)), 3138 (ν(C−H)), 2216 m (ν(C≡C)), 1612 s (ν(C═N)), 1500 w, 1430 w (ν(C═C)), 1255 vs, 1226 s (ν(C−F)), 1166 s (ν(S−O)), 1060 m, 1030 vs, 835 m, 797 m, 759 m, 682 m, 639 vs, 573 m, 551 m, 518 m, 478 m, 278 w, 254 m. ^{1}H NMR (270 MHz, DMSO-d_6) δ_H (ppm) 8.81 (brs, α-Py(**1t**)), 8.69 (d, J = 6.72 Hz, β-Py(**1d**)), 7.87−7.69 (m), 7.62 (t, 5-*Ph* (**1t**)), 5.71 (brs, NH_2 (**1d**)), 5.57 (brs, NH_2 (**1t**)), 2.67 (brs, CH_2 (**1t**, **1d**)). ^{13}C{H} NMR δ_C (ppm) 151.88 (α-Py), 135.17 (C_6H_4), 133.75 (*ipso*-Py), 129.97 (C_6H_4), 127.96 (β-Py), 123.03 (C_6H_4), 121.31 (C_6H_4), 118.28 (C_6H_4), 96.20 (C≡C), 86.26 (C≡C), 46.78 (CH_2). ^{19}F NMR (465.89 MHz, DMSO-d_6) δ_F (ppm) −79.13. CSI-MS (DMF, 263 K) m/z 2085.78 (calcd m/z 2085.98). Anal. Calcd for $C_{72}H_{72}F_{18}N_{12}O_{24}Pd_3S_6$ ($[(en)Pd(L)]_3(OTf)_6\cdot 6H_2O$): C, 36.91; H, 3.11; N, 7.17. Found: C, 37.18; H, 3.09; N, 6.75.

Synthesis of $[(en^*)Pd(L)]_n(PF_6)_{2n}$ 2t/2d·PF_6 (2t, n = 3; 2d, n = 2). The starting material $(en^*)PdCl_2$ (0.0524 g, 0.178 mmol) was dissolved in MeCN (10 mL) followed by the addition of 2 equiv of $AgPF_6$ (0.0904 g, 0.357 mmol). After the solution was stirred for 4 h, the resulting AgCl was removed by filtration. The bridging ligand 1,3-bis(4-pyridylethynyl)benzene (0.0502 g, 0.178 mmol) was added to the filtrate, and the mixture was stirred overnight. The solvent was then removed by evaporation, and the crude product was dissolved in nitromethane. Finally, the residual solid was centrifuged and recrystallized from nitromethane/Et_2O to give pale-green crystals of **2d·PF_6** (0.0874 g, 0.0551 mmol, 61.9% yield). IR (KBr, cm^{-1}) 3655 m, 3587 m, 3108 w, 2994 w, 2930 w, 2858 w, 2216 m (ν(C≡C)), 1611 s (ν(C═C and C═N)), 1558 w, 1501 m, 1473 m, 1431 m, 1297 w, 1214 m, 1169 w, 1124 w, 1065 m, 1042 w, 1007 w, 955 m, 839 vs (ν(P−F)) 768 m, 738 m, 683 w, 557 s. ^{1}H NMR (500 MHz, DMSO-d_6) δ_H (ppm) 9.19 (d, J = 6.90 Hz, α-Py(**2t**)), 9.15 (d, J = 6.60 Hz, α-Py(**2d**)), 7.84 (d, J = 6.90 Hz, β-Py(**2t**)), 7.82 (d, J = 6.60 Hz, α-Py(**2d**)), 7.79 (brs, 2-C_6H_4(**2t**)), 7.78 (brs, 2-C_6H_4(**2d**)), 7.72 (d, J = 8.00 Hz, 4-C_6H_4(**2t**)), 7.68 (d, J = 8.00 Hz, 4-C_6H_4(**2d**)) 7.60 (t, J = 8.00 Hz (m, 5-C_6H_4(**2t**)), 7.59 (t, J = 8.00 Hz (m, 5-C_6H_4(**2d**)), 3.01 (brs, CH_2 (**2d**)), 2.99 (brs, CH_2 (**2t**)) 2.64 (s, Me(**2d**)), 2.57 (s, Me(**2t**)). ^{13}C{H}NMR (124.50 MHz, DMSO-d_6) δ_C (ppm) 151.13 (α-Py(**2t**)), 150.04 (α-Py(**2d**)), 133.73 (*ipso*-Py), 132.30 (C_6H_4)), 128.76 (C_6H_4), 121.26 (*ipso*-C_6H_4), 121.18 (*ipso*-C_6H_4), 96.44 (C≡C), 86.23 (C≡C (**2t**)), 85.63 (C≡C (**2d**)), 62.19 (CH_2), 50.41 (Me(**2d**)), 50.29 (Me(**2t**)). ^{31}P{H} NMR (109.25 MHz, DMSO-d_6) δ_p (ppm) −142.95 (sept, J_{P-F} = 387.83 Hz). ^{19}F NMR (465.89 MHz, DMSO-d_6) δ_F (ppm) −71.51 (d, J_{P-F} = 711.60 Hz, PF_6^-). CSI-MS (DMF, 263 K) m/z 1441.04 (calcd m/z 1440.79). Anal. Calcd for $C_{52}H_{60}O_2N_8P_4F_{24}Pd_2$ ($[(en^*)Pd(L)]_2(PF_6)_4\cdot 2H_2O$): C, 38.51; H, 3.73; N, 6.91. Found: C, 38.57; H, 3.89; N, 6.89.

Synthesis of $[(dppe)Pd(L)(OTf)_2]_\infty$ 3·OTf. The compound $(dppe)Pd(OTf)_2$ (0.321 g, 0.357) was reacted with 1,3-bis(4-pyridylethynyl)benzene (0.100 g, 0.357 mmol) in CH_2Cl_2 (20 mL) for 1 h. After the solution was concentrated by evacuation, the addition of *n*-hexane produced $\{(dppe)Pd(L)(OTf)_2\}_\infty$ (0.368 g, 0.340 mmol) as a yellow solid in 95% yield. ^{1}H NMR (500 MHz, DMSO-d_6) δ_H (ppm) 8.67 (d, $^3J_{H-H}$ = 6.30 Hz, *Py*(α)), 7.82 − 7.78 (m, *m-Ph* (dppe), 5-C_6H_4), 7.72 (t, $^3J_{H-H}$ = 7.75 Hz, *p-Ph* (dppe)), 7.68 (dd, $^3J_{H-H}$ = 7.68 Hz, $^3J_{H-H}$ = 1.15 Hz, 4,6-C_6H_4), 7.60 (ddd, $^3J_{H-P}$ = 7.45 Hz, $^4J_{H-H}$ = 7.75 Hz, $^3J_{H-H}$ = 1.15 Hz, *o-Ph*), 7.57 (d, $^3J_{H-H}$ = 6.30 Hz, Py(β)), 7.57 (d, $^3J_{H-H}$ = 7.68 Hz, 2-C_6H_4), 3.09 (d, $^2J_{H-P}$ = 23.75 Hz, CH_2). ^{13}C{H} NMR (124.50 MHz, DMSO-d_6) δ_C (ppm) 150.34 (*Py*(α)), 134.97 (5-C_6H_4), 133.32 (d, $^3J_{C-P}$ = 10.7 Hz, *m-Ph*), 133.27 (*p-Ph*), 132.94 (2-C_6H_4), 129.90 (4,6-C_6H_4), 129.55 (d, J = 11.8 Hz, *o-Ph* (dppe)), 127.49 (*Py*(β)), 125.62 (d, $^2J_{C-P}$ = 56.0 Hz, *ipso-Ph*), 124.58 (brs, *p*-C_6H_4),121.37 (*ipso-Py*), 120.70 (q, $^2J_{C-F}$ = 321.86 Hz, CF_3SO_3), 95.52, 86.38 (C≡C), 27.23 (d, J_{C-P} = 40.52 Hz, CH_2). ^{31}P{H} NMR (200.43 MHz, DMSO-d_6) δ_P (ppm) 68.31. ^{19}F NMR (465.89 MHz, DMSO-d_6) δ_F (ppm) −79.18. CSI-MS (MeCN, 263 K) m/z 934.09 (calcd m/z 934.23). A single crystal was obtained as the hexatungstate derivative of $\{[(dppe)Pd(L)][W_6O_{19}]\}_\infty$ by recrystallization from DMSO/acetone. Anal. Calcd for $C_{46}H_{36}O_{19}N_2P_2PdW_6$ ($\{[(dppe)Pd(L)][W_6O_{19}]\cdot 6H_2O\}_\infty$: C, 24.02; H, 2.10; N, 1.02. Found: C, 23.98; H, 2.17; N, 0.99. The reproducibility of the formation of **3·W_6O_{19}** as single crystals was checked four times by NMR (purity ≥99%).

Diffusion Ordered NMR Spectroscopy (DOSY). DOSY NMR measurements were carried out at 303 K using bipolar pulse pair longitudinal eddy current delay (BPP-LED) for ^{1}H and ^{19}F nuclei and bipolar pulse pair stimulated echo (BPP-STE) pulse sequences for ^{1}H and ^{31}P nuclei. The diffusion (Δ s) and gradient times (δ ms) and the gradient control (0.05−0.27 [T/m]) were carefully controlled for the respective measurements. Curve-fitting analyses were carried out with the JEOL Delta 5.0.2 program and the data were fit to eq 1, where I is the observed intensity, I_0 is the observed intensity without gradients, γ is the gyromagnetic ratio of the observed nucleus, δ is the length of the gradient pulse, G is the gradient strength, Δ (diffusion delay) is the delay between the midpoints of the gradients, and D is the diffusion coefficient.

$$\ln\left(\frac{I}{I_0}\right) = -(\gamma\delta)^2\left(\Delta - \frac{\delta}{3}\right)DG^2 \quad (1)$$

dx.doi.org/10.1021/ic401428v | *Inorg. Chem.* 2013, 52, 11200−11209

Encapsulation of $[\alpha\text{-}PW_{12}O_{40}]^{3-}$ with 2t/2d·PF_6. Compound **2t/2d·PF_6** (20.0 mg, 8.41 μmol as the molecular hexagon) and 1 equiv of $H_3[\alpha\text{-}PW_{12}O_{40}]$ (24.2 mg, 8.41 μmol) were dissolved in 0.75 mL of DMSO-d_6 following which ^{1}H and ^{31}P DOSY NMR spectra were obtained at 303 K. The resulting solution was then diluted with DMF, and CSI-MS measurement was performed at 263 K. Molecular dynamics calculations were performed with universal force field (UFF) parameters using the Forcite algorithm within the Materials Studio software package. Elemental analysis was carried out on the nitrate derivative, $[(en^*)Pd(L)]_3[\alpha\text{-}PW_{12}O_{40}](NO_3)_3\cdot 2DMF\cdot 5H_2O$. Anal. Calcd for $C_{84}Pd_3W_{12}H_{102}O_{56}N_{17}P$: C, 21.00; H, 2.14; N, 4.96. Found: C, 21.29; H, 2.55; N, 4.67. IR (KBr, cm^{-1}): 3093 w, 3004 w, 2912 w (ν(C−H)), 2215 m (ν(C≡C)), 1611 s (ν(C═C) and ν(C═N)), 1533 w, 1498 w, 1470 w, 1430 m, 1384 m (ν(C−N)), 1320 w, 1217 w, 1080 vs, 1041 m, 1027 m, 1006 m, 977 vs, 896 s, 816 vs, (ν(W═O), ν(P═O), and ν(W−O−W)), 683 m, 666 w, 595w, 571 w, 549 w, 953 m, 389 s, 337 w, 302 w, 265 m, 254 m.

Single-Crystal X-ray Crystallography. Diffraction measurements of **1t·OTf**, **2d·PF_6**, and **3·W_6O_{19}** were obtained using a Rigaku MicroMax-007 with Mo Kα radiation (λ = 0.71069 Å). A total of six and four anion molecules of **1t·OTf** and **2d·PF_6** were apparently observed, but were highly disordered. As a result, the disordered anions and solvents were squeezed and removed from the structural solution. Details concerning the crystallographic analysis are provided in the Supporting Information. CCDC 942775 (**1t·OTf**), 942776 (**2d·PF_6**), and 942777 (**3·W_6O_{19}**) contain the crystallographic data, and these data can be obtained free of charge from the Cambridge Crystallographic Data Centre via www.ccdc.cam.ac.uk/conts/retrieving.html.

■ ASSOCIATED CONTENT

Supporting Information

X-ray crystallography and DFT calculation details. Crystallographic data in CIF format. IR spectra of **1t·OTf**, **2d·PF_6**, **3·OTf**, and $[(en^*)Pd(L)]_3[\supset\alpha\text{-}PW_{12}O_{40}](NO_3)_3$. CSI-MS spectrum of **3·OTf**. ^{1}H, ^{13}C, and ^{19}F NMR spectra of **1t·OTf**, **2d·PF_6**, and **3·OTf**. ^{1}H DOSY spectra and/or curve fitting analyses of **1t/1d·OTf**, **2t/2d·PF_6**, **3·OTf**, **2t/2d·PF_6** in the presence of $H_3[\alpha\text{-}PW_{12}O_{40}]$, **2t·**$[\alpha\text{-}PW_{12}O_{40}]^{3-}$, **2d·**$[\alpha\text{-}PW_{12}O_{40}]^{3-}$, and $H_3[\alpha\text{-}PW_{12}O_{40}]$. Complete citation for ref 30. This material is available free of charge via the Internet at http://pubs.acs.org.

■ AUTHOR INFORMATION

Corresponding Author

*E-mail: tmizuno@mail.ecc.u-tokyo.ac.jp. Phone: +81-3-5841-7272. Fax: +81-3-5841-7220.

Notes

The authors declare no competing financial interest.

■ ACKNOWLEDGMENTS

This work was supported by Grants-in-Aid for Scientific Research, Ministry of Education, Culture, Science, Sports and Technology of Japan (MEXT) and the Funding Program for World-Leading Innovative R&D on Science and Technology (FIRST Program) of the Japan Society for the Promotion of Science (JSPS).

■ REFERENCES

(1) (a) Lehn, J.-M. *Supramolecular Chemistry*; VCH: New York, 1995. (b) Haiduc, I.; Edelmann, F. T. *Supramolecular Organometallic Chemistry*; Wiley-VCH: Weinheim, Germany, 1999. (c) Steed, J. W.; Atwood, J. L. *Supramolecular Chemistry*, 2nd ed.; John Wiley & Sons: Chichester, United Kingdom, 2009.

(2) (a) O'Keeffe, M.; Yaghi, O. M. *Chem. Rev.* **2012**, *112*, 675−702. (b) Fujita, M.; Tominaga, M.; Hori, A.; Therrien, B. *Acc. Chem. Res.* **2005**, *38*, 371−380. (c) Férey, G.; Mellot-Draznieks, C.; Serre, C.; Millange, F. *Acc. Chem. Res.* **2005**, *38*, 217−225. (d) Steel, P. J. *Acc. Chem. Res.* **2005**, *38*, 243−250. (e) Kitagawa, S.; Matsuda, R. *Coord. Chem. Rev.* **2007**, *251*, 2490−2509. (f) Férey, G. *Chem. Soc. Rev.* **2008**, *37*, 191−214. (g) Young, N. J.; Hay, B. P. *Chem. Commun.* **2013**, *49*, 1354−1379.

(3) (a) Kim, K.; Selvapalam, N.; Ko, Y. H.; Park, K. M.; Kim, D.; Kim, J. *Chem. Soc. Rev.* **2007**, *36*, 267−279. (b) Pinalli, R.; Dalcanale, E. *Acc. Chem. Res.* **2013**, *46*, 399−411. (c) Nishikiori, S.; Yoshikawa, H.; Sano, Y.; Imamoto, T. *Acc. Chem. Res.* **2005**, *38*, 227−234. (d) Lerouge, M. H.; Hudhomme, P.; Sallé, M. *Chem. Soc. Rev.* **2011**, *40*, 30−43. (e) Safont-Sempere, M. M.; Fernández, G.; Würthner, F. *Chem. Rev.* **2011**, *111*, 5784−5814. (f) Chen, B.; Xiang, S.; Qian, G. *Acc. Chem. Res.* **2010**, *43*, 1115−1124. (g) Bradshaw, D.; Claridge, J. B.; Cussen, E. J.; Prior, T. J.; Rosseinsky, M. J. *Acc. Chem. Res.* **2005**, *38*, 273−282. (h) Hardouin-Lerouge, M.; Hudhomme, P.; Sallé, M. *Chem. Soc. Rev.* **2011**, *40*, 30−43. (i) Pluth, M. D.; Raymond, K. N. *Chem. Soc. Rev.* **2007**, *36*, 161−171.

(4) (a) Chen, B.; Xiang, S.; Qian, G. *Acc. Chem. Res.* **2010**, *43*, 1115−1124. (b) Suh, M. P.; Cheon, Y. E.; Lee, E. Y. *Coord. Chem. Rev.* **2008**, *252*, 1007−1026. (c) Struzhkin, V. V.; Militzer, B.; Mao, W. L.; Mao, H.; Hemley, R. J. *Chem. Rev.* **2007**, *107*, 4133−4151. (d) Zhao, D.; Timmons, D. J.; Yuan, D.; Zhou, H.-C. *Acc. Chem. Res.* **2011**, *44*, 123−133. (e) Ward, M. D. *Science* **2003**, *300*, 1104−1105.

(5) (a) Horcajada, P.; Charati, T.; Serre, C.; Gillet, B.; Sebrie, C.; Baati, T.; Eubank, J. F.; Heutaux, D.; Clayette, P.; Kreuz, C.; Chang, J.-S.; Hwang, Y. K.; Marsaud, V.; Bories, P.-N.; Cynober, L.; Gil, S.; Férey, G.; Couvreur, P.; Gref, R. *Nat. Mater.* **2010**, *9*, 172−178. (b) Thematic issues on drug delivery based on supramolecule: Issacs, L. *Adv. Drug Delivery Rev.* **2012**, *64*, 763. (c) Paolino, D.; Cosco, D.; Molinaro, R.; Celia, C.; Fresta, M. *Drug Discovery Today* **2011**, *16*, 311−324.

(6) Yoon, M.; Srirambalaji, R.; Kim, K. *Chem. Rev.* **2012**, *112*, 1196−1231.

(7) (a) Ruben, M.; Rojo, J.; Romero-Salguero, F. J.; Uppadine, L. H.; Lehn, J.-M. *Angew. Chem., Int. Ed.* **2004**, *43*, 3644−3662. (b) Zhang, W.; Xiong, R.-G. *Chem. Rev.* **2012**, *112*, 1163−1195.

(8) Tashiro, K.; Aida, T.; Zheng, J.-Y.; Kinbara, K.; Saigo, K.; Sakamoto, S.; Yamaguchi, K. *J. Am. Chem. Soc.* **1999**, *121*, 9477−9478.

(9) Thematic issues on anion species concerning supramolecules: (a) Gale, P. A.; Gunnlaugsson, T. *Chem. Soc. Rev.* **2010**, *39*, 3595−3596. (b) Gale, P. A. *Chem. Commun.* **2011**, *47*, 82−86. (c) Arunachalam, M.; Ghosh, P. *Chem. Commun.* **2011**, *47*, 8477−8492. (d) Davis, J. T.; Okunola, O.; Quesada, R. *Chem. Soc. Rev.* **2010**, *39*, 3843−3862. (e) Ballester, P. *Chem. Soc. Rev.* **2010**, *39*, 3810−3830. (f) Juwarker, H.; Jeong, K.-S. *Chem. Soc. Rev.* **2010**, *39*, 3664−3674.

(10) (a) Stang, P. J.; Olenyuk, B. *Acc. Chem. Res.* **1997**, *30*, 502−518. (b) Leininger, S.; Olenyuk, B.; Stang, P. J. *Chem. Rev.* **2000**, *100*, 853−908. (c) Amijs, C. H. M.; van Klink, G. P. M.; van Koten, G. *J. Chem. Soc., Dalton Trans.* **2006**, 308−327. (d) Zangrando, E; Casanova, M.; Alessio, E. *Chem. Rev.* **2008**, *108*, 4979−5013. (e) Fujita, M.; Sasaki, O.; Mitsuhashi, T.; Fujita, T.; Yazaki, J.; Yamaguchi, K.; Ogura, K. *J. Chem. Soc., Chem. Commun.* **1996**, 1535−1536.

(11) (a) Volkringer, C.; Popov, D.; Loiseau, T.; Guillou, N.; Férey, G.; Haouas, M.; Taulelle, F.; Mellot-Draznieks, C.; Burghammer, M.; Riekel, C. *Nat. Mater.* **2007**, *6*, 760−764. (b) Ouellette, W.; Wang, G.; Liu, H.; Yee, G. T.; O'Connor, C. J.; Zubieta, J. *Inorg. Chem.* **2009**, *48*, 953−963. (c) Yang, J.; Marendaz, J.-L.; Geib, S. J.; Hamilton, A. D. *Tetrahedron Lett.* **1994**, *35*, 3665−3668. (d) Rashidi, M.; Jennings, M. C.; Puddephatt, R. J. *Chem. Eng. Commun.* **2003**, *5*, 65−66.

(12) (a) Yamamoto, T.; Anf, A. M.; Stang, P. J. *J. Am. Chem. Soc.* **2003**, *125*, 12309−12317. (b) Stang, P. J.; Persky, N. E.; Manna, J. *J. Am. Chem. Soc.* **1997**, *119*, 4777−4778. (c) Hasenknopf, B.; Lehn, J.-M.; Boumediene, N.; Dupont-Gervais, A.; Dorsselaer, A. V.; Kneisel, B.; Fenske, D. *J. Am. Chem. Soc.* **1997**, *119*, 10956−10962. (d) Newkome, G. R.; Cho, T. J.; Moorefield, C. N.; Baker, G. R.; Cush, R.; Russo, P. S. *Angew. Chem., Int. Ed.* **1999**, *38*, 3717−3721. (e) Rucareanu, S.; Mongin, O.; Schuwey, A.; Hoyler, N.; Gossauer, A. *J. Org. Chem.* **2001**, *66*, 4973−4988. (f) Deng, H.; Grunder, S.; Cordova, K. E.; Valente, C.; Furukawa, H.; Hmadeh, M.; Gándara, F.;

Whalley, A. C.; Liu, Z.; Asahina, S.; Kazumori, H.; O'Keeffe, M.; Terasaki, O.; Stoddart, J. F.; Yaghi, O. M. *Science* **2012**, *336*, 1018−1023.
(13) (a) Fujita, M.; Yazaki, J.; Ogura, K. *J. Am. Chem. Soc.* **1990**, *112*, 5645−5647. (b) Fujita, M.; Yazaki, J.; Ogura, K. *Tetrahedron Lett.* **1991**, *32*, 5589−5592.
(14) (a) Schweiger, M.; Seidel, S. R.; Arif, A. M.; Stang, P. J. *Angew., Chem., Int. Ed.* **2001**, *40*, 3467−3469. (b) Schweiger, M.; Seidel, R.; Arif, A. M.; Stang, P. J. *Inorg. Chem.* **2002**, *41*, 2556−2559.
(15) Lai, S.-W.; Chan, M. C.-W.; Peng, S.-M.; Che, C.-W. *Angew. Chem., Int. Ed.* **1999**, *38*, 669−671.
(16) (a) Schnebeck, R.-D.; Freisinger, E.; Glahé, F.; Lippert, B. *J. Am. Chem. Soc.* **2000**, *122*, 1381−1390. (b) Willermann, M.; Mulcahy, C.; Sigel, R. K. O.; Cerdà, M. M.; Freisinger, E.; Miguel, P. J. S.; Roitzsch, M.; Lippert, B. *Inorg. Chem.* **2006**, *45*, 2093−2099.
(17) Carina, R. F.; Williams, A. F.; Bernardinelli, G. *Inorg. Chem.* **2001**, *40*, 1826−1832.
(18) Yu, S.-Y.; Huang, H.-P.; Li, S.-H.; Jiao, Q.; Li, Y.-Z.; Wu, B.; Sei, Y.; Yamaguchi, K.; Pan, Y.-J.; Ma, H.-W. *Inorg. Chem.* **2005**, *44*, 9471−9488.
(19) (a) Ferrer, M.; Gutiérrez, A.; Mounir, M.; Rossell, O.; Ruiz, E.; Rang, A.; Engeser, M. *Inorg. Chem.* **2007**, *46*, 3395−3406. (b) Ferrer, M.; Mounir, M.; Ruiz, E.; Maestro, M. A. *Inorg. Chem.* **2003**, *42*, 5890−5899.
(20) Derossi, S.; Casanova, M.; Lengo, E.; Zangrando, E.; Stener, M.; Alessio, E. *Inorg. Chem.* **2007**, *46*, 11243−11253.
(21) Weilandt, T.; Troff, R. W.; Saxell, H.; Rissanen, K.; Schalley, C. A. *Inorg. Chem.* **2008**, *47*, 7588−7598.
(22) Lee, S. B.; Hwang, S.; Chung, D. S.; Yun, H.; Hong, J.-I. *Tetrahedron Lett.* **1998**, *39*, 873−876.
(23) (a) Uehara, K.; Kasai, K.; Mizuno, N. *Inorg. Chem.* **2007**, *46*, 2563−2570. (b) Uehara, K.; Kasai, K.; Mizuno, N. *Inorg. Chem.* **2010**, *49*, 2471−2478.
(24) (a) Thematic issues on polyoxometalate: Hill Ed, C. *Chem. Rev.* **1998**, *98*, 1. (b) *Polyoxometalate Chemistry for Nano-Composite Design*; Yamase, T., Pope, M. T., Eds.; Kluwer: Dordrecht, The Netherlands, 2002. (c) Kozhevnikov, I. V. *Catalysis by Polyoxometalates*; Wiley: Chichester, United Kingdom, 2002. (d) Pope, M. T. In *Comprehensive Coordination Chemistry II*; Wedd, A. G., McCleverty, J. A., Meyer, T. J., Eds.; Elsevier: Boston, MA, 2004; Vol. *4*, p 635. (e) Hill, C. L. In *Comprehensive Coordination Chemistry II*; Wedd, A. G., McCleverty, J. A., Meyer, T. J., Eds.; Elsevier: Boston, MA, 2004; Vol. *4*, p 679. (f) Neumann, R. In *Modern Oxidation Methods*; Bäckvall, J. E., Ed.; Wiley-VCH: Weinheim, Germany, 2004; p 223. (g) Yu, R.; Kuang, X.-F.; Wu, X.-Y.; Lu, C.-Z.; Donahue, J. P. *Coord. Chem. Rev.* **2009**, *253*, 2872−2890.
(25) (a) The encapsulation of POMs in cages in the solid state: Hagrman, P. J.; Hagrman, D.; Zubieta, J. *Angew. Chem., Int. Ed.* **1999**, *38*, 2638−2684. and references therein. (b) Férey, G.; Mellot-Draznieks, C.; Serre, C.; Millage, F.; Dutour, J.; Surblé, S.; Margiolaki, I. *Science* **2005**, *309*, 2040−2042. (c) Sun, C.-Y.; Liu, S.-X.; Liang, D.; Ren, Y.-H.; Su, Z.-M. *J. Am. Chem. Soc.* **2009**, *131*, 1883−1888. (d) Kuang, X.; Wu, X.; Yu, R.; Donahue, J. P.; Huang, J.; Lu, C.-Z. *Nat. Chem.* **2010**, *2*, 461−465. (e) Nohra, B.; Moll, H. E.; Albelo, L. M. R; Mialane, P.; Marrot, J.; Mellot-Draznieks, C.; O'Keeffe, M.; Biboum, R. N.; Lemaire, J.; Keita, B.; Nadjo, L.; Dolbecq, A. *J. Am. Chem. Soc.* **2011**, *133*, 13363−13374. (f) Fu, H.; Qin, C.; Lu, Y.; Zhang, Z.-M.; Li, Y.-G.; Su, Z.-M.; Li, W.-L.; Wang, E.-B. *Angew., Chem., Int. Ed.* **2012**, *51*, 7985−7989.
(26) (a) Pregosin, P. S.; Kumar, P. G. A.; Fernández, I. *Chem. Rev.* **2005**, *105*, 2977−2998. (b) Allouche, L.; Marquis, A.; Lehn, J.-M. *Chem.—Eur. J.* **2006**, *12*, 7520−7525. (c) Zheng, Y.-R.; Ghosh, K.; Stang, P. J. *Inorg. Chem.* **2010**, *49*, 4747−4749. (d) Jiang, H.; Lin, W. *J. Am. Chem. Soc.* **2006**, *128*, 11286−11297. (e) Pluth, M. D.; Tiedemann, B. E. F.; van Halbeek, H.; Nunlist, R.; Raymond, K. N. *Inorg. Chem.* **2008**, *47*, 1411−1413. (f) Martínez-Viviente, E.; Pregosin, P. S.; Vial, L.; Herse, C.; Lacour, J. *Chem.—Eur. J.* **2004**, *10*, 2912−2918. (g) Ferrer, M.; Pedrosa, A.; Rodríguez, L.; Rossell, O.; Vilaseca, M. *Inorg. Chem.* **2010**, *49*, 9438−9449.
(27) (a) Chan, Y.-T.; Li, X.; Yu, J.; Carri, G. A.; Moorefield, C. N.; Newkome, G. R.; Wesdemiotis, C. *J. Am. Chem. Soc.* **2011**, *133*, 11967−11976. (b) Avram, L.; Cohen, Y. *J. Am. Chem. Soc.* **2005**, *127*, 5714−5719. (c) Megyes, T.; Jude, H.; Grósz, T.; Bakó, I.; Radnai, T.; Tárkányl, G.; Pálinkás, G.; Stang, P. J. *J. Am. Chem. Soc.* **2005**, *127*, 10731−10738. (d) Allouche, L.; Marquis, A.; Lehn, J.-M. *Chem.—Eur. J.* **2006**, *12*, 7520−7525. (e) Oliva, A. I.; Gómez, K.; González, G.; Ballester, P. *New. J. Chem.* **2008**, *32*, 2159−2163. (f) Cavarzan, M.; Scarso, A.; Sgarbossa, P.; Strukul, G.; Reek, J. N. H. *J. Am. Chem. Soc.* **2011**, *133*, 2848−2851.
(28) (a) Floquet, S.; Brun, S.; Lemonnier, J.-F.; Henry, M.; Deisuc, M.-A.; Prigent, Y.; Cadot, E.; Taulelle, F. *J. Am. Chem. Soc.* **2009**, *131*, 17254−17259. (b) Lemonnier, J.-F.; Floquet, S.; Kachmar, A.; Rohmer, M.-M.; Bénard, M.; Marrot, J.; Terazzi, E.; Piguet, C.; Cadot, E. *J. Chem. Soc., Dalton Trans.* **2007**, 3043−3054. (c) Lokeren, L. V.; Cartuyvels, E.; Absillis, G.; Wilem, R.; Parac-Vogt, T. N. *Chem. Commun.* **2008**, 2774−2776. (d) Schäffer, C.; Bögge, H.; Merca, A.; Weinstock, I. A.; Rehder, D.; Haupt, E. T. K.; Müller, A. *Angew. Chem., Int. Ed.* **2009**, *48*, 8051−8056.
(29) Preliminary single-crystal X-ray crystallography of **3·OTf** also confirmed the formation of the infinite chain compound $\{[(dppe)Pd(L)](OTf)_2\}_\infty$. In addition, we have reported that the steric repulsion between the supporting (*N*,*N*,*N*′,*N*′-tetramethylethylenediamine, en*) and bridging ligands (pyradine, Pyr) prevented the formation of both the molecular triangle and square, $[(en^*)Pd(Pyr)(NO_3)_2]_n$ (n = 3, 4), and that the infinite chain compound $[(en^*)Pd(Pyr)(NO_3)_2]_\infty$ was formed.[23b]
(30) Frisch, M. J.; et al. *Gaussian09*, revision B.01; Gaussian, Inc.: Wallingford, CT, 2009.
(31) Tomasi, J.; Mennucci, B.; Cammi, R. *Chem. Rev.* **2005**, *105*, 2999−3094.
(32) Johnson, A. M.; Moshe, O.; Gamboa, A. S.; Langloss, B. W.; Limtiaco, F. K.; Larive, C. K.; Hooley, R. J. *Inorg. Chem.* **2011**, *50*, 9430−9442.
(33) (a) Wojciechowski, W.; Matczak-jon, E. *Inorg. Chim. Acta* **1990**, *173*, 85−91. (b) Djuran, M. I.; Milinkovic, S. U. *Polyhedron* **2000**, *19*, 959−963. (c) Jenkins, J. M.; Verkade, J. G. *Inorg. Synth.* **1968**, *11*, 108.